

## **Two-dimensional Seismic Wave Modeling and Inversion by the Boundary Element Method**

S. Bignardi<sup>1</sup>, F. Fedele<sup>2</sup>, A. J. Yezzi<sup>3</sup>, G. J. Rix<sup>4</sup>  
and G. Santarato<sup>5</sup>

<sup>1</sup>University of Ferrara, Earth sciences Department, Via Saragat 1, Ferrara, Italy; PH 349-6595142; email: bgnsml@unife.it

<sup>2</sup>School of Civil and Environmental Engineering and School of Electrical and Computer Engineering, Georgia Institute of Technology, USA; PH (912)966-6785; email: fedele@gatech.edu

<sup>3</sup>School of Electrical and Computer Engineering, Georgia Institute of Technology, USA; PH (404)385-1017; email: yezzi@ece.gatech.edu

<sup>4</sup>School of Civil and Environmental Engineering, Georgia Institute of Technology, USA; PH (404)894-2292; email: glenn.rix@ce.gatech.edu

<sup>5</sup>University of Ferrara, Earth sciences Department., Via Saragat 1, Ferrara, Italy; PH 0532-974728; email: giovanni.santarato@unife.it

### **ABSTRACT**

Surface wave methods (SWM) are widely used for the geophysical characterization of geological bodies and tectonic structures in both Earth Sciences and Engineering. SWMs exploit the dispersive nature of Rayleigh waves to indirectly estimate shear wave velocity profiles from surface wave measurements, but they are limited to parallel-layered geometries. To overcome such limitations, we exploit the Boundary Element Method (BEM) to define a new class of geometric inversion models that allows to go directly from raw measurements to estimating the shape of laterally varying soil interfaces. The proposed approach enables a robust identification of the subsurface geometry and it aims at filling the gap between the standard simplistic parallel-layered-based SWM and the more complex three-dimensional Full Wave Inversion (FWI) based on Finite Element Methods. Numerical tests on synthetic data unveil the effectiveness of the inverse algorithm and its applicability to wave measurements. An application to field data is finally presented.

### **INTRODUCTION**

Subsurface mechanical characterization is a crucial issue in many fields of both Earth Sciences and Geotechnical Engineering. Indeed, good knowledge of geological conditions is fundamental for seismic hazard assessment, seismic microzonation, foundation and building design. Besides the use of direct investigations, such as drilling or excavations, which yield pointwise information and are expensive even at the metric-to-decametric scale, common alternative methods include the analysis of active or passive seismic waves. In recent years SWM have been widely used for near-surface characterization, especially for the estimation of the velocity  $V_s$  of  $S$ -waves at depths of 30 m or so, as  $V_s$  directly relates to the soil stiffness at small

strain levels. SWMs utilize the dispersive nature of Rayleigh waves in a heterogeneous half space to obtain  $V_s$  from surface wave particle motions excited and recorded on the ground surface. There are now many variations of the basic test and inversion protocol, including the original Spectral Analysis of Surface Waves (Nazarian et al. 1984; Stokoe et al. 1994), multi-channel array methods (Tselentis and Delis 1998; Park et al. 1999) and passive techniques (Louie, 2001; Park et al., 2005) to enrich data in the low-frequency band in order to increase information at greater depths. Recently, wave attenuation has been modeled in the parameter inversion and soil damping ratios can be estimated as well (Rix et al. 2001, Lai et al. 2002). SWMs usually assume Rayleigh waves propagating through a stack of horizontal, isotropic and homogenous soil layers. Such models are well established and computationally efficient (Aki and Richards 1980); however, they only capture the vertical variation of elastic properties, viz. they are one dimensional (1-D). Further, the flat-layered model is only an approximation of the geometry of realistic sites, and it may yield misleading results if the actual soil is far from the assumed flat geometry. Indeed, the major drawback is that wave propagation is modeled as the linear superposition of dispersive Rayleigh modes in parallel layered media, which cannot describe the scattered wave-field when strong lateral variations occur. Observations and modeling of earthquakes confirm, for example, that seismic waves can be amplified at alluvial valley edges, and diffraction effects can be observed because the interface between soft sediments and bedrock is far from being horizontal (Bard and Gabriel 1986). Furthermore, surface topography can alter seismic wave propagation (Bard 1982, Raptakis et al. 2000). In particular, amplification is usually expected at hill tops (Bard 1982) and complex amplified and de-amplified patterns occur at hill flanks (Savage 2004).

There have been several attempts to include lateral variations via the so-called "pseudo-2-D" inversion (e.g. Luo et al. 2008, Boiero and Socco 2010), in which data along the survey line are windowed and successive 1-D inversions are combined by means of suitable blending kernels. However, this approach still retains the 1-D approximation of SWMs and can only capture details on a scale comparable to the extent of the spatial window used for inversion. As a result, only weak layer variations can be observed. Analytical solutions for two-dimensional (2-D) media are available only for a very restricted class of weakly varying geometries (Maupin 2007; Dravinski and Mossessian 1997). As such, these solutions are of limited practical value. The further maturation of SWMs has been thus limited by the lack of robust and efficient computational methods that enable more realistic soil representations, even in three-dimensions (3-D). Recently, for crustal and lithospheric scale structures, such limitations have been overcome by a FWI methodology which combines a robust forward model based on Higher Order Finite Element Method (FEM) and adjoint techniques (Komatitsch, 1998; Fichtner, 2010). When a FEM forward model is used, complex media are finely discretized into 3-D elements by a large number of nodes. Each node is associated with a set of unknown parameters that characterize the mechanical properties of the soil at that node. Typically, the number of parameters exceeds the number of measurements available by several orders of magnitude, and thus the inverse problem is severely ill-posed. Ill-posedness is usually treated by regularization procedures. The shortcoming is that these approaches suffer from problems of slow convergence and are computationally intensive.

In this paper, we propose an alternative inversion formulation based on BEM that overcomes the above-mentioned limitations of FEM-based FWIs, and at the same time exploits a far more realistic modeling than the current state-of-the-art SWMs (Bignardi et al, 2011). The proposed approach aims at filling the gap between the standard simplistic parallel-layered-based SWM and the more complex 3-D FEM-based FWI, enabling a robust and better geometric characterization of soil subsurfaces. Here, the focus is in identifying the geometry of strongly varying interfaces in layered media. In particular, wave propagation for the forward model is solved by BEM (Dominguez 1993), which is an effective technique for soil media whose properties can be considered as regionally homogenous. Indeed, BEM was previously exploited to solve problems concerning structural vibration analysis, transient waves, and dynamics of cavities under the influence of body or surface waves (Manolis and Beskos 1983; Beskos et al. 1986) and to investigate the propagation of seismic waves in laterally varying layered media (Dineva and Manolis 2001b). The approach is restricted to the frequency domain and the soil parameters are assumed known, but they can be easily estimated together with the geometric properties of the subsurface. This joint inversion will be discussed elsewhere. The paper is structured as follows: we first outline the analytical formulation of the 2-D forward model and the associated numerical solution. Then, the associated inverse problem is introduced to infer the subsurface interface geometry. Finally, applications to benchmark problems and to a set of experimental data are presented.

## BEM-BASED FORWARD MODEL

Consider monochromatic waves at frequency  $\omega$  propagating through a 2-D layered subsurface, as shown in Figure 1(a). Let  $\Omega_j$  be the generic layer bounded by

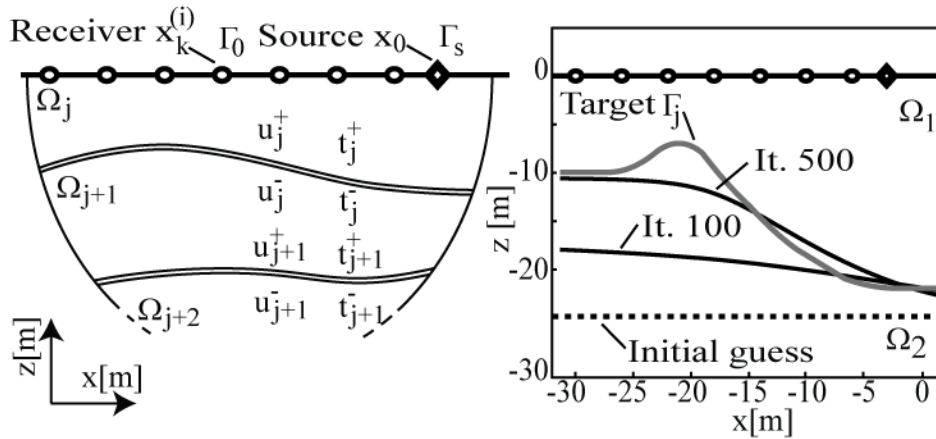


**Figure 1: (a) Model setup and (b) BEM-based inversion of a two-layered media.**

the curve  $\Gamma = \Gamma_{j-1} \cup \Gamma_j$ , and  $x$  and  $z$  are horizontal and vertical coordinates, respectively. In the frequency domain, the wave propagation problem in the  $j$ -th layer can be reformulated in the integral form (Beskos et al. 1986)

$$\int_{\Gamma} \mathbf{U}^{(j)}(\mathbf{x}, \mathbf{s}, \omega) \mathbf{t}_{j(\mathbf{N})}(\mathbf{x}, \omega) d\Gamma = \int_{\Gamma} \mathbf{T}^{(j)}(\mathbf{x}, \mathbf{s}, \omega) \mathbf{u}_j(\mathbf{x}, \omega) d\Gamma + \mathbf{C} \mathbf{u}_j(\mathbf{x}, \omega), \quad \mathbf{x} \in \Gamma.$$

Continuity of displacements and stresses at the layer interfaces requires that

$$\mathbf{u}_j^+(\mathbf{x}, \omega) = \mathbf{u}_j^-(\mathbf{x}, \omega), \quad \mathbf{t}_{j(\mathbf{N}^+)}^+(\mathbf{x}, \omega) = -\mathbf{t}_{j(\mathbf{N}^-)}^-(\mathbf{x}, \omega), \quad \mathbf{x} \in \Gamma_j, \quad (1)$$

where  $+/-$  signs refer to the values calculated with respect to the upper and lower layers adjacent to the interface  $\Gamma_j$ , and  $\mathbf{N}$  is the outward normal. Further, vanishing normal stress  $\mathbf{t}_{0(\mathbf{N})}^-$  must be enforced at the free surface  $\Gamma_0$  except at the source location  $\mathbf{x}_0 \in \Gamma_s$  where  $\mathbf{t}_{0(\mathbf{N})}^- = f_0(\omega) \delta(\mathbf{x} - \mathbf{x}_0) \mathbf{N}$ ,  $f_0$  being the Fourier amplitude of the load along the normal to the surface and  $\delta(\mathbf{x})$  is the Dirac function. The fundamental tensors  $\mathbf{U}^{(j)}$  and  $\mathbf{T}^{(j)}$  are given in Dominiguez (1984), and they depend upon the elastic parameters of the layer  $j$ , that is the density  $\rho_j$ , shear modulus  $\mu_j$ , Poisson's ratio  $\nu_j$  and unit source location  $\mathbf{s}$ . The  $(2 \times 2)$  tensor  $\mathbf{C}$  accounts for singular contributions to the influence matrix terms at the element's nodes and for energy conservation in infinite piecewise domains (Dominiguez 1993). The BEM approximation is obtained by discretizing each interface  $\Gamma_j$  in  $e_j$  quadratic isoparametric elements along which the field values of displacements and stresses are given by

$$\mathbf{u}_j(\mathbf{x}) = \sum_{n=1}^3 P_n(\eta) \mathbf{u}_{k,n}^{(j)}, \quad \mathbf{t}_{j(\mathbf{N})}(\mathbf{x}) = \sum_{n=1}^3 P_n(\eta) \mathbf{t}_{k,n}^{(j)}, \quad \mathbf{x} \in \Gamma_{j,k}, \quad (2)$$

where  $\mathbf{u}_{k,n}^j$  and  $\mathbf{t}_{k,n}^j$  are vectors of displacements and stresses at the  $n^{\text{th}}$  node on the  $k^{\text{th}}$  element  $\Gamma_{j,k}$ , and  $P_n(\eta)$  are interpolating functions with  $\eta \in [-1, 1]$ . Using (2) and cycling the point of application of fundamental tensors on all node positions, a system of linear equations for the layer  $j$  is obtained

$$[\mathbf{K}^{(j)}] \{\mathbf{u}^{(j)}\} = [\mathbf{G}^{(j)}]^{-1} [\mathbf{H}^{(j)}] \{\mathbf{u}^{(j)}\} = \{\mathbf{t}^{(j)}\}, \quad (3)$$

where the matrices  $[\mathbf{G}^{(j)}]$ ,  $[\mathbf{H}^{(j)}]$  are given in Beskos (1986) and the vectors  $\{\mathbf{u}^{(j)}\}$  and  $\{\mathbf{t}^{(j)}\}$  list displacements and tensions at the boundary nodes, respectively. These are local degrees of freedom (dof). Equations (3) are assembled by imposing the matching conditions (1) as in Beskos (1986). The resulting linear system can be written in compact form as

$$[\mathbf{K}] \mathbf{u}_g = \mathbf{t}_g, \quad (4)$$

where  $\mathbf{u}_g$ ,  $\mathbf{t}_g$  are global dof. The solution of (4) follows after imposing free surface and source conditions. Weight drop or sledge hammer sources are modeled in Fourier space as a nodal tension vector of intensity  $f_0(\omega)$  acting perpendicular to the soil surface. For massive sources, such as an electro-mechanical shaker, the generated stress at the ground surface is given by  $\mathbf{t}_s = m\omega^2 \mathbf{d}_s + \mathbf{F}$ , where the vectors  $\mathbf{F}$  and  $\mathbf{d}_s$  represent the shaker's force and displacements at the source boundary portion  $\Gamma_s$  and  $m$  is the shaker's mass. We point out that BEM can be easily generalized to multi-frequency wave propagation in 3-D geometries and viscoelasticity can be

accounted for by the correspondence principle (Christensen, 1971; Manolis, 1981).

## GEOMETRIC BEM-BASED WAVE INVERSION

Assume that the Fourier amplitudes  $\mathbf{u}_{d_k}(\omega)$  of the vector displacements are known from measurements using  $N_{rec}$  receivers at  $\mathbf{x}_k^{(r)} \in \Gamma_0$ ,  $k = 1, \dots, N_{rec}$ . We consider an equispaced discretization for the interface  $\Gamma_j$  along  $\hat{\mathbf{x}}$  using  $n_l$  nodes. The shape of  $\Gamma_j$  can be inferred directly from the measured data by minimizing the energy functional

$$\mathcal{E}(\Gamma_j) = \frac{1}{2} \sum_{r=1}^{N_{Rec}} \|\mathbf{u}_k - \mathbf{u}_{d_k}\|^2 + \alpha \sum_{n=1}^{N_{int}} \sum_{k=1}^{e(n)} \int_{-1}^1 \left[ \left( \frac{\partial x_k^{(i)}}{\partial \eta} \right)^2 + \left( \frac{\partial z_k^{(i)}}{\partial \eta} \right)^2 \right]^{\frac{1}{2}} d\eta. \quad (5)$$

The first term represents the mismatch  $E$  between measurements and theoretical displacements at the receivers based on the forward model (4). The second term is an arc-length regularizer to treat ill-posedness when  $n_l > 2N_{rec}$ ,  $N_{int}$  is the number of interfaces to be estimated and  $e(n)$  is the number of elements of the  $k^{\text{th}}$  interface. The optimal deformation of the interface  $\Gamma_j$  that makes the first variation of the energy  $\mathcal{E}$  vanish is obtained by the following iterative algorithm. Firstly, we recall that each interface  $\Gamma_j$  is discretized using  $n_j$  nodes with coordinates given by  $\Gamma_j^{(0)} = (x_j^{(i)}, z_{0,j}^{(i)})$ . To minimize  $\mathcal{E}$  we restrict the deformation of the curve along the vertical direction  $\hat{\mathbf{z}}$ , i.e., we change the nodal coordinate  $z_j$  only. To do so, set

$$z_j^{(i)} = z_{0,j}^{(i)} + \Delta_{z,j} \quad \Delta_{z,j} \ll z_{0,j}^{(i)},$$

where  $z_{0,j}$  defines an initial guess and  $\Delta_{z,j}$  is a small perturbation. Taylor-expanding (5) to first order with respect to  $\Delta_{z,j}$  yields the optimal deformation  $\Delta_z$  as a solution of the linear system of equations

$$([\mathbf{J}][\mathbf{J}]^T + \alpha[\mathbf{R}])\{\Delta_z\} = -[\mathbf{J}]\{\mathbf{u}_{k_0} - \mathbf{u}_{d_k}\} - \alpha\{\mathbf{q}\}, \quad (6)$$

where  $\Delta_z$  is a column vector that lists the vertical perturbations  $\Delta_{z,j}$ ,  $[\mathbf{J}]$  is the the Jacobian matrix that measures the changes of the wave displacements at the receivers due to changes of the interface  $\Gamma_j^{(0)}$ , the superscript  $T$  denotes the conjugate transpose and the matrix entries in  $[\mathbf{R}]$  and  $\{\mathbf{q}\}$  are given in Bignardi et al. (2011). Given an initial guess  $\Gamma_j^{(0)}$  of the unknown interface  $\Gamma_j$ , the energy (5) is minimized by iteratively evolving the initial interface according to (6) until the error  $e = \max(|\Delta_{z,j}|)$  is smaller than a given tolerance  $\varepsilon$ . Relaxation is introduced to limit the increments  $\Delta_{z,j}$  at each iteration by penalizing the squared norm of  $\{\Delta_z\}$ . This adds an extra term  $\beta[\mathbf{I}]$  to the left-hand side of (6), where  $[\mathbf{I}]$  is the identity matrix and  $\beta$  is a fixed constant. The weight  $\alpha$  is initially chosen 10 to 30 times larger than the value  $\alpha_0$  that equally weights misfit ( $M$ ) and regularizer ( $R$ ), viz.  $M = \alpha_0 R$ , so that

the algorithm reconstructs the large-scale features of the curve. As the error  $e$  reduces,  $\alpha$  is decreased at a constant rate allowing the identification of smaller scale features.

## APPLICATIONS

**Synthetic data.** Consider the two-layered subsurface profile of Figure 1(b) and a typical SWM instrumentation setup. The receivers are equispaced every four meters, and the source is located three meters away from the closest receiver. We assume to know the source and the elastic characteristics of the two layers. Data at the receivers, which are simulated using the BEM-based forward model (4), consist of Fourier amplitudes of both vertical and horizontal displacements. At this first stage, no noise is added to the data since we wish to test the convergence of the algorithm to the exact target interface. In particular, the algorithm converges to the exact interface in approximately 1500 iterations and some of the intermediate iterates are also shown in Figure 1(b). To test the algorithm's performance using data corrupted with 5 to 10% random gaussian noise, we consider two data sets. The first set defines a soil configuration of a high acoustic impedance contrast and elastic parameters given by  $V_s = 150(800) \text{ m/s}$ ,  $V_p = 500(2000) \text{ m/s}$  and  $\rho = 1600(2200) \text{ Kg/m}^3$  for the upper (lower) layer, respectively,  $V_p$  being the velocity of  $P$ -waves. The second set, conversely, represents a low impedance contrast configuration and  $V_s = 150(250) \text{ m/s}$ ,  $V_p = 500(1000) \text{ m/s}$  and  $\rho = 1600(2000) \text{ Kg/m}^3$ . Further, the source intensity is  $f_0(\omega) = 1000N$  at frequency  $\omega = 1 \text{ rad/s}$ . If noise is added to the simulated measurements, the algorithm still converges as clearly shown in Figure 2(a) for both

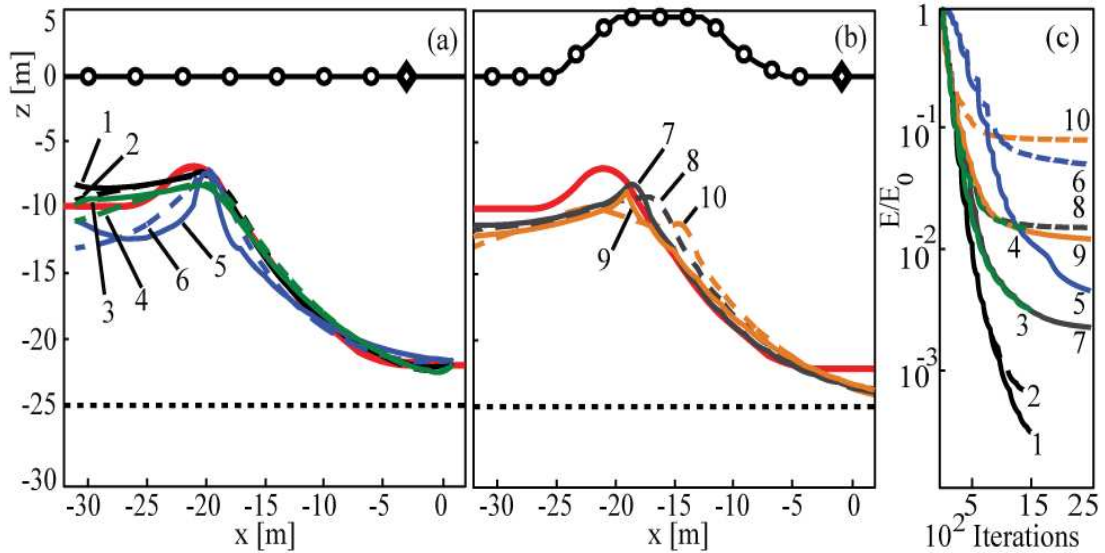


**Figure 2: (a), High/low acoustic impedance jump inversions of 5% noisy data. (b), Case of 10% noise with irregular topography and (c), normalized misfit  $E/E_0$ .**

the high (curves 1,2) and low (3,4) acoustic impedance cases. Further, in Figure 2(c) we also show the normalized misfit  $E/E_0$  as a function of the number of iterations,  $E_0$  being the misfit of the initial estimate. In particular, the algorithm is more sensitive to noise in the phases (dashed curves) rather than amplitudes (solid curves). Note that the 5-10% level noise added to the Fourier amplitudes corresponds to an even larger error in the associated time-based displacements due to the nature of the Fourier transform. In Figure 2(a), curves (5,6) denote the converged interfaces when horizontal measurements are discarded. The algorithm is effective in identifying the major features of the target interface even using only half of the data. In such conditions, the  $\alpha$  parameter is decreased at slower rate and  $\beta$  is increased to assure better convergence. Finally, the algorithm can also handle irregular ground surfaces in a natural manner as clearly illustrated in Figure 2(b).

**Field-case study.** We inverted a set of experimental data collected by SWM testing at a site in Alabama in 2004. The source was an electromechanical shaker operated as a harmonic source in order to generate signals with frequencies ranging from about 3 to 100 Hz. Only vertical particle accelerations were measured by means of a linear array of 15 low-frequency accelerometers located at distances ranging from 2.4 to 32 meters from the source as shown in Figure 3(a).

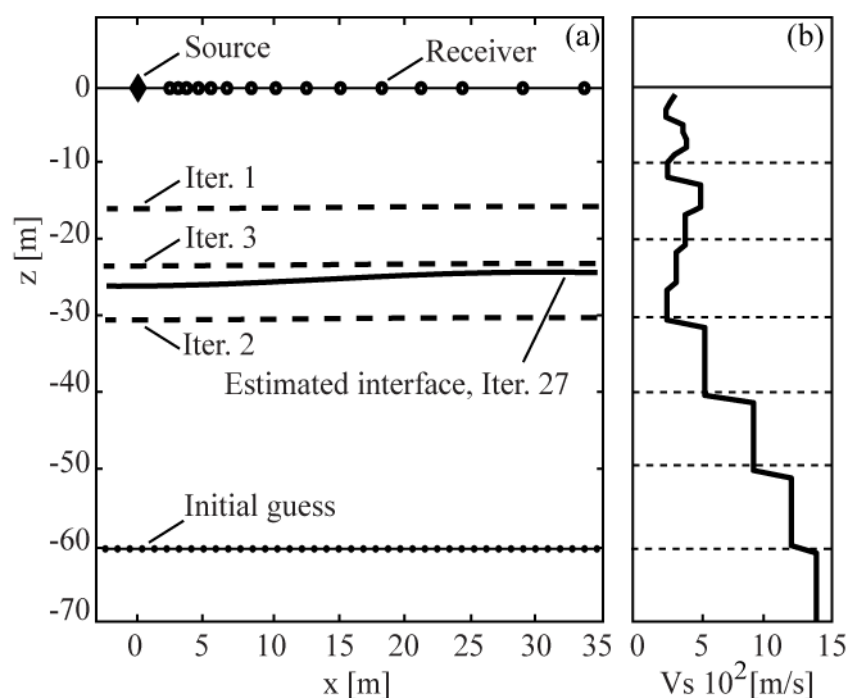


**Figure 3: (a) Inversion of experimental data. (b)  $V_s$  profile from classical SWM**

Time-series were Fourier-transformed, integrated and then compared with the expected displacements. Conventional 1-D SWM inversions performed at various locations of the site suggest a two-layered subsurface structure which is uniform in the horizontal direction. For example, Figure 3(b) shows one of the estimated

vertical profiles of the shear velocity. Further, the elastic parameters of the two layers are estimated using a standard inversion based on the BEM forward model (4) assuming parallel layers. In particular, for the upper (lower) layer given by  $V_s = 335(1369)m/s$ ,  $V_p = 664(2001)m/s$  and  $\rho = 1500(2400)Kg/m^3$ . We intentionally apply our BEM algorithm to test if it is capable of identifying a parallel layered structure from the data set. As a result, the algorithm converged in 27 iterations and a two-layered media subsurface is revealed as shown in Figure 3(a) where we also report some of the intermediate iterates of the inversion. Observe that the convergence occurs by rigid translations, clearly indicating that the algorithm is capable of accurately determining the position of a flat interface as a limiting case.

## CONCLUSIONS.

We introduced a geometric inversion formulation that overcomes the limitations of classic SWMs in dealing with laterally varying subsurface layers. The proposed inverse algorithm exploits BEM to model wave propagation through a 2-D layered subsurface and infers the shape of the interface between two layers directly from measurements at the receivers. Tests on both synthetic and experimental data provide evidence that the BEM-based geometric inversion is robust to noise and it is applicable to geometries with steep interfaces or irregular free surfaces. Furthermore, the BEM-solution can be exploited as the initial guess for FEM-based FWIs in order to reconstruct higher-order structured heterogeneities and improve the robustness and accuracy of the FEM-based solution. We believe that the application of BEM-based inverse models to geological problems will enable researchers and other stakeholders to investigate the underground geological complexities with a low-cost method. Our preliminary results are very promising in that we are able to identify an irregular interface in a 2-D layered model. The approach is in principle scale-invariant and has no space limitations. Work is in progress to extend it to multi-frequency and 3-D geometries.

## REFERENCES.

- Aki, K., and Richards P.G.(2002). *Quantitative Seismology, Theory and Methods*, second edition, University Science Books, Sausalito, California.
- Bard, P.Y. (1982). "Diffracted waves and displacement field over two-dimensional elevated topographies." *Geophys. J. R. astr. Soc.*, **71**, 731-760.
- Bard, P.Y., and Gabriel, J.C. (1986). "The seismic response of two-dimensional sedimentary deposits with large vertical velocity gradients." *Bull. Seism. Soc. Am.*, **76**, 343-366.
- Beskos, D.E., Leung, K.L., and Vardoulakis, I.G. (1986). "Vibration Isolation of Structures From Surface Waves in Layered Soil." *Rec. Appl. Comput. Mech.*, 125-140.
- Bignardi, S. (2011). *Complete waveform inversion approach to seismic surface waves and adjoint active surfaces*. Ph.D. dissertation at the University of Ferrara
- Bignardi, S., Fedele, F., Rix, G.J., Yiezzi, A. J., and Santarato, G. (2011). "Geometric seismic wave inversion by the boundary element method." *Bull. Seism. Soc.*



- Am.*, In print.
- Boiero, D., and Socco, V. (2010). "Retrieving lateral variations from surface wave dispersion curves." *Geophys. Prospect.*, 58,221-233.
- Dineva, P., and Manolis, G. (2001b) "Scattering of seismic waves by cracks in multi-layered geological regions: II. Numerical results." *Soil Dyn. Earthq. Eng.*, 21,627-641.
- Dominguez, J., (1993). *Boundary elements in dynamics*, Computational Mechanics Publications, Elsevier, Southampton, London.
- Dravinski, M., and Mossessian, T.K. (1997). "Scattering of Plane Harmonic P,SV and Rayleigh Waves by Dipping Layers of Arbitrary Shape." *Bull. Seism. Soc. Am.*, 77(1), 212-235.
- Fichtner, A. (2010). *Full seismic waveform modelling and inversion*, Springer-Verlag, Heidelberg.
- Komatitsch, D., and Vilotte, J.P. (1998). "The spectral-element method: an efficient tool to simulate the seismic response of 2D and 3D geological structures." *Bull. Seismol. Soc. Am.*, 88(2), 368-392.
- Lai, C.G., Rix, G.J., Foti, S., and Roma, V. (2002). "Simultaneous measurement and inversion of surface wave dispersion and attenuation curves." *Soil Dyn. Earthq. Eng.*, 22(9-12), 923-930.
- Louie, J. N. (2001). "Faster, better: shear-wave velocity to 100 meters depth from refraction microtremor arrays." *Bull. Seism. Soc. Am.*, 91(2), 347-364.
- Luo, Y.H., Xia, J.H., Liu, J.P., Xu, Y.X., and Liu, Q.S. (2008). "Generation of a pseudo-2D shear-wave velocity section by inversion of a series of 1D dispersion curves." *J. Appl. Geophys.*, 64, 115-124.
- Manolis, G.D., and Beskos, D.E. (1983). "Dynamic response of lined tunnels by an isoparametric boundary element method." *Comput. Methods Appl. M.*, 36(3), 291-307.
- Maupin, V. (2007). "Introduction to mode coupling methods for surface waves." *Adv. Geophys.*, 48, 127-155.
- Nazarian, S., and Stokoe, K.H. (1984). "In situ shear wave velocity from spectral analysis of surface waves, *Proc. 8<sup>th</sup> Conference on Earthquake engineering*, St. Francisco, Prentice Hall, 3, 31-38.
- Park, C.B., Miller, R.D., and Xia, J. (1999). "Multichannel analysis of surface waves." *Geophysics*, 64, 800-808.
- Park, C.B., Miller, R.D., Ryden, N., Xia, J., and Ivanov, J. (2005). "Combined use of active and passive surface waves" *J. Env. Eng. Geophys.*, 10, 323-334.
- Raptakis, D., Chavez-Garcia, F. J., Makra, K., and Pitilakis, K. (2000). "Site effects at Euroseistest-I. Determination of the valley structure and confrontation of observations with 1D analysis." *Soil Dyn. Earthq. Eng.*, 19(1), 1-22.
- Rix, G.J., Lai, C.G., and Foti, S. (2001). "Simultaneous Measurement of Surface Wave Dispersion and Attenuation Curves." *Geotech. Test. J.*, 24(4), 350-358.
- Savage, W.Z. (2004). "An Exact Solution for Effects of Topography on Free Rayleigh Waves." *Bull. Seism. Soc. Am.*, 94(5), 1706-1727.
- Stokoe, K.H., Wright, S.G. Bay, J.A., and Roesset, J.M. (1994). "Characterization of geotechnical sites by SASW method." *Proc.that show convergence to the target interface. No noise added to simulated XIII Int. Conf. on Soil Mechanics*

- and Foundation Engineering*, Oxford & IBH Publishing, New Delhi, 15-25.
- Tselentis, G.A., and Delis, G. (1998). "Rapid assessment of S-wave profiles from the inversion of multichannel surface wave dispersion data." *Annali di Geofisica*, 41, 1-15.
- Virieux, J., and Operto, S. (2009). "An overview of full-waveform inversion in exploration geophysics." *Geophysics*, 74(6), 127-152.